# Alternant conjugated oligomers with tunable and narrow HOMO–LUMO gaps as sustainable nanowires

**ARTICLE** *in* RSC ADVANCES · DECEMBER 2013

Impact Factor: 3.84 · DOI: 10.1039/C3RA41572D



**2 AUTHORS:**

Sergio Manzetti
Fjordforsk AS
**47** PUBLICATIONS **210** CITATIONS
SEE PROFILE

Tian Lu
Beijing Kein Research Center for Natural Sc…
**31** PUBLICATIONS **863** CITATIONS
SEE PROFILE

RSC Advances

RSC Publishing

PAPER

# Alternant conjugated oligomers with tunable and narrow HOMO–LUMO gaps as sustainable nanowires†

Cite this: *RSC Adv.*, 2013, **3**, 25881

Sergio Manzetti[ab] and Tian Lu*[ac]

Novel nanowire technologies encompass the use of metals and crystals with a high electric transport potential and superior charge-collection properties. However, nanowires built on metals such as cadmium, gallium-arsenide and similar alloys present serious environmental and health risks. The use of carbon is a far more environmentally friendly solution than heavy-metal based nanowires, and if arranged in a particular manner, it can provide excellent conductive properties that are applicable in nanowire technologies. Herein, we report an investigation into the particular carbon-based $4n/4n + 2$ alternant resonance, which has the potential of becoming a key component for the design of novel and conductive nanomaterials, suitable for application in optoelectronics, nanoelectronics and microelectronics. A set of nine $4n/4n + 2$ oligomers comprising in the range of 15–20 cyclic units (~5 nm) were analyzed quantum mechanically. The results show that the number and type ($4n$ or $4n + 2$) of carbon-rings (cyclobutadiene, benzene and naphthalene) that constitute the oligomers, govern the HOMO–LUMO gaps with a statistical relevance of $R^2 = 0.919$. Interestingly, we found that the sequence of the units played a central role in shaping the conductance of the $4n/4n + 2$ oligomers, and that the sequencing of units in conductive carbon-based oligomers can be a potential future approach in tailoring the gaps of carbon-based conductive components for application in molecular electronics devices. An interesting relationship was also found between the symmetry and the homo- and heteromorphism of the LUMO elements with the HOMO–LUMO gaps, suggesting a pattern of continuity and wavefunction-symmetry across the LUMO orbitals of the $4n/4n + 2$ systems to be a key-element determining the narrow gaps in the conductive carbon oligomers. In addition, population and electrostatic potential analysis showed that π-electron distribution over the oligomers is quite non-uniform. The electron delocalization behavior over the $4n$ and $4n + 2$ rings was characterized by electron localization function, six-center bond order, and a striking linear relationship was found between the π-delocalization index of the C–C bonds and the HOMO–LUMO gaps ($R^2 = 0.988$). The results presented herein introduce valuable approaches and data for the engineering of conductive materials to be applied in the field of nanoelectronics and microelectronics, and to relieve the development of nanowires from its dependence on expensive and rare metals.

Received 2nd April 2013
Accepted 1st October 2013

DOI: 10.1039/c3ra41572d

**www.rsc.org/advances**

## 1 Introduction

Nanowires are nano-sized conducting wires used in modern solar-cell technologies, micro- and nanoelectronic circuits, and other novel energy-harvesting technologies. Their excellent versatility lies in their high charge-collection and charge-transport properties, as well as their light-absorption properties through light-trapping.[1–3] Recent developments in nanowire technology include the use of nanocircuits and nanosensors to compose solid structures that are 40–200 nm in diameter, an example of which is cadmium sulphide and copper sulphide nanowires connected in series or parallel configurations.[4] Such nanowires are important components in future computing and electronic devices, and can be engineered in a complex manner with silicon units for application in nanotransistors, energy storage units and batteries, and they have also recently been applied in current third generation energy-harvesting technologies.[5]

However, nanowires built with cadmium, gallium-arsenide and other heavy metals present serious environmental threats and health-risks.[6] Such solid nanowires also have a slow degree of transformation in their life cycle and also involve health-risks during their fabrication process.[7] Carbon however, is a far more

[a]*Fjordforsk Institute of Science and Technology, Fresvik, 6896 Norway; Web: http://www.fjordforsk.no. E-mail: sergio.manzetti@fjordforsk.no; sobereva@sina.com*

[b]*Computational Systems and Biology, Biomedical Centre, University of Uppsala, Sweden*

[c]*Department of Chemistry and Chemical Engineering, School of Chemical and Biological Engineering, University of Science and Technology Beijing, Beijing 100083, P. R. China*

† Electronic supplementary information (ESI) available. See DOI: 10.1039/c3ra41572d

environmentally friendly solution than heavy-metal based nanowires, and is known from recent and older studies to have metallic properties if arranged in a proper fashion.[8–11] Additionally, large carbon molecules and polymers are biodegradable,[12,13] and have also been demonstrated to exhibit semiconducting and superconducting properties.[8,10,14,15] In some of these experiments, MacDiarmid and colleagues[8,14,15] introduced a carbon-polymer rationale which can be the basis of their suitability for application in nanowire technologies, by showing that quasi-linear carbon-based molecular architectures can function as molecular wires if organized in a specific fashion. Some sustainable carbon-based materials and polymers have already been explored recently for conducting purposes in plastic optoelectronics,[16] and also for hydrogen storage purposes.[17] However, the metallic (charge-transferring) nature of carbon, as described extensively by Alcarazo,[18] has still not been applied in linear single-chained carbon-based nanowire-structures analogous to conventional metal-based nanowires, and has rather been applied to conductive nanocomposites and thin films.[8,14,15,19]

The drawback of such technologies is that thin films are difficult, if not impossible to reduce to single-chain conductive units, in order to supersede the thin diameters of metal-nanowires (less than 20 nm diameter), and they can therefore be difficult to use in the development of single-chain oligomers for conducting electricity at the nanoelectronic level. Also, the films and nanocomposites have considerable disadvantages over metal-based nanowires in terms of their susceptibility to oxidants, an issue which is suggested to have been circumvented through the different approach of applying the oligomers presented herein.[20]

In other words, the quest for carbon-based nano-sized single-chained polymers/oligomers is still in its infancy, and rigorous studies on the chemical, physical and electronic properties of carbon in various oligomeric and polymeric arrangements are needed.

In this context, we introduce the $4n/4n + 2$ system as a novel approach to tunable linear conductive carbon-based materials. Alternant conjugated $4n/4n + 2$ systems exhibit different electronic properties from conventional conjugated π-systems due to the merging of anti-aromatic and aromatic energy levels in the same molecule.[21] Such energy transitions within the same molecule can play a valuable role in low-voltage conductive technologies, giving rise to the potential for tuning the electronic signals across the molecule by virtue of the number of anti-aromatic and aromatic sections on the molecule. Interestingly, previous quantum chemical studies on small alternant $4n/4n + 2$ systems performed by Aoki *et al.*[22] showed non-trivial relationships between the HOMO–LUMO energies and orbital coefficients. Alternant $4n/4n + 2$ systems have also been found to have extremely high HOMO energies and extremely low LUMO energies, and to be key structures in voltammetry studies.[23] We report a group of $4n/4n + 2$ alternant conjugated oligomers (Fig. 1) and a detailed study of their electronic properties, in addition to statistical correlations between their anti-aromatic/aromatic content and gap widths. In this study we also report a detailed wavefunction analysis of these systems, which reveals intriguing properties for the development of carbon-based tunable oligomers, such as the effect of monomer sequence order. With respect to the need for carbon-based conductive technologies as described above, the $4n/4n + 2$ resonance system therefore represents a potentially useful rationale for "green" nanowire technologies and can aid the scientific community in tailoring alternatives to heavy-metal based nanowires.

The results presented herein are therefore intended to shift scientific focus from metal-based nanowires to carbon-based technologies, to advance research into sustainable and tunable novel conductive materials.

## 2 Materials and methods

Nine oligomers with alternating conjugation were drawn and prepared for analysis using GabEdit and Gaussview[24,25] (see Fig. 1).

The structure optimizations were performed using the Gaussian 03 package,[25] and the density functional (DFT) method B3LYP[26] with the 6-31G* basis-set.[27,28] Based on these optimized geometries, the HOMO–LUMO gaps were calculated using the DFT methods B3LYP, B3PW91,[29] BHandLYP,[26] PBE[30] and mPWPW91,[31] in conjunction with the 6-31G* basis-set. In order to assess the influence of basis-set, the gaps were also evaluated at the B3LYP/6-31+G(2d,p)[32] level.

Statistical analysis was performed with the software XPlot,[33] using a confidence interval of 95%.

Based on the wavefunctions at the B3LYP/6-31G* level, all wavefunction analyses were carried out with the program Multiwfn, version 3.1.[34] Population numbers of π-electrons were derived using the Mulliken method.[35] Atomic charges were derived using the atomic dipole corrected Hirshfeld (ADCH) method,[36] and it was shown that ADCH atomic charge is capable of faithfully reflecting charge distribution, possessing a good ability to reproduce electrostatic potential.[37] Delocalization index (DI)[38] was originally proposed for the AIM atomic basin,[39] however to facilitate the calculation, we calculated DI in Becke's fuzzy atomic space, and this is equivalent to fuzzy bond order.[40] The orthonormality of σ and π orbitals allows DI to be exactly separated into DI-σ and DI-π. The calculation of multicenter bond order followed its definition, which is given in ref. 41, but the constant prefactor was ignored.

## 3 Results and discussion

### 3.1 Calculated HOMO–LUMO gaps

It is well known that B3LYP/6-31G* is capable of producing a quite satisfactory gap for conjugated polymers,[42–44] and therefore the gaps for oligomers A–I were all calculated at this level and are reported in Fig. 1. The corresponding wavefunctions were subjected to the analyses presented in later sections.

In order to assess the influence of the DFT functionals on the oligomer gaps, with the same basis-set 6-31G*, the gaps were also calculated using two generalized gradient approximation (GGA) functionals, PBE[30] and mPWPW91,[31] as well as another two hybrid functionals, B3PW91[29] and BHandHLYP.[26] Note that the Hartree–Fock (HF) exchange component in BHandHLYP is

 

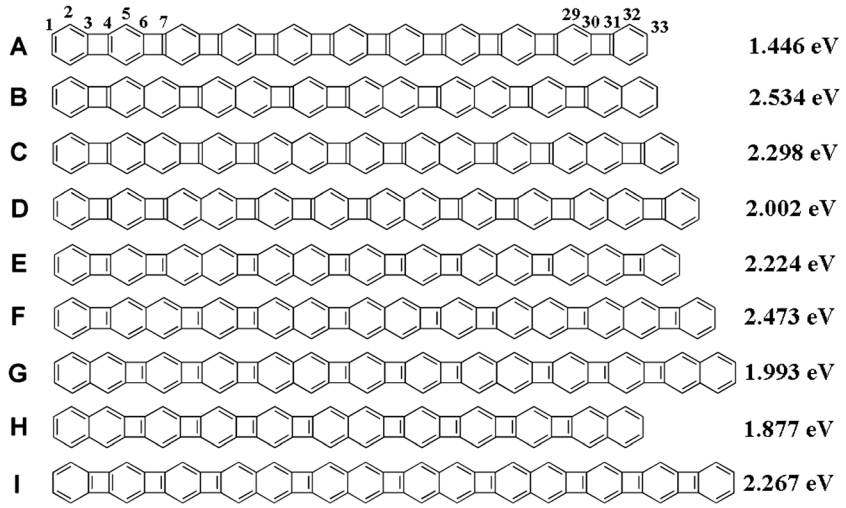


**Fig. 1** Nine oligomers of alternating conjugated resonance. Calculated HOMO–LUMO gaps at the B3LYP/6-31G* level are reported on the right for each oligomer. The carbon atoms of each oligomer are numbered from left to right, as shown for oligomer A.

as high as 50%, while it is only 20% in both B3LYP and B3PW91. To examine the influence of the basis-set, B3LYP was also used to evaluate the gaps in conjunction with a larger basis-set 6-31+G(2d,p). The results are plotted in Fig. 2.

From Fig. 2 one can see that regardless of which functional or basis-set is used, the relative gaps between the different oligomers are basically identical, suggesting that the gap order of the oligomers A–I is definitive. The absolute values of the gaps almost solely depend on the HF component in the DFT functionals. Both sets of gaps predicted by PBE and mPWPW91 are consistently lower than the B3LYP gaps by about 1.0 eV. The gaps yielded by B3LYP and B3PW91 are essentially the same. BHandHLYP consistently overestimated the gaps by about 1.7 eV in comparison to B3LYP, mainly due to its very high HF component. The quality of the basis-set only trivially affects the gaps; using 6-31+G(2d,p) instead of 6-31G* lowered the gaps by about 0.07 eV.

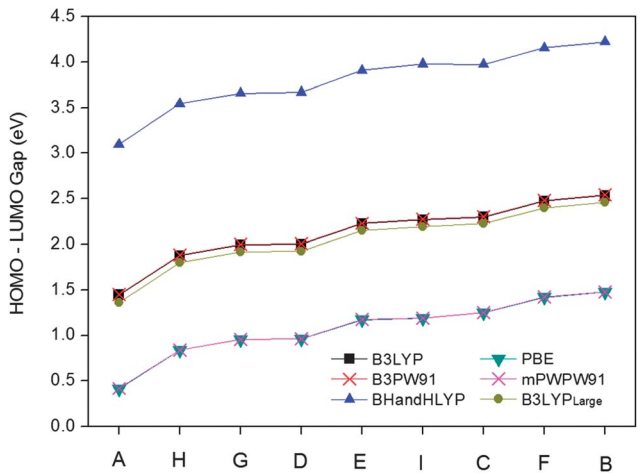


**Fig. 2** The HOMO–LUMO gaps of the oligomers A–I, calculated by various DFT functionals in combination with the 6-31G* basis-set. The $B3LYP_{Large}$ corresponds to the gaps calculated at the B3LYP/6-31+G(2d,p) level.

We note that the order of molecular orbitals, in particular the shapes of the HOMO and LUMO, do not rely on the choice of DFT functional and basis-set. Therefore the discussions on the HOMO and the LUMO in the following sections are free of ambiguity.

The energetic separation between the HOMO and the HOMO − 1, as well as between the LUMO and the LUMO + 1, were also examined by using various DFT functionals and basis-sets for the nine oligomers (see Fig. S1 and S2 in ESI†). From the figures one can see that the energetic separation is clearly different from oligomer to oligomer, and that the smallest separation occurs in oligomer I. However, even in the case of oligomer I, the LUMO and LUMO + 1, and especially the HOMO and HOMO − 1 are still not degenerated. As with the calculated gaps, the separation degrees are only evidently influenced by the HF component in the DFT functionals. This influence is consistent for the separation between the HOMO and the HOMO − 1, but probably due to the fact that virtual orbitals have relatively unclear physical meaning, the influence on the energetic difference between the LUMO and the LUMO − 1 is somewhat complex.

### 3.2 Relationship between the HOMO–LUMO gap and chemical composition

The nine $4n/4n + 2$ conjugated alternant systems were investigated by a statistical analysis of their HOMO–LUMO gap widths, as done previously for other carbon materials.[45] The anti-aromatic units, namely the cyclobutadienes ($4n$), were systematically interchanged with the classical π-chemistry of the benzene and naphthalene units ($4n + 2$) in alternative sequences, resulting in different combinations of the anti-aromatic and aromatic chemistries in the oligomers sized 4–6 nm in length (see Fig. 1). The statistical analyses showed that two quadratic regressions described the statistically significant relationship between the HOMO–LUMO gap and the chemical

composition of the oligomers (see Fig. 3 and Table 1). The first regression relates the crude $4n/4n+2$ content to the gaps

$$\text{Gap (eV)} \approx 5.148x^2 - 10.521x + 6.753 \text{ with } R^2 = 0.919 \quad (1)$$

where $x$ is the $4n/4n+2$ ratio in the oligomer, *e.g.* oligomer A has ten $4n$ units and eleven $4n+2$ units, therefore $x = 10/11 = 0.909$.

The second regression applies a simple relationship between all units (cyclobutadiene, benzene, and naphthalene) to the HOMO–LUMO gaps of the oligomers

$$\text{Gap (eV)} \approx -25.261x^2 + 10.495x + 1.463 \text{ with } R^2 = 0.929 \quad (2)$$

where $x$ denotes the ratio calculated by dividing the number of naphthalene units by the number of benzene units and then dividing again by the number of cyclobutadiene units (napht./benz./cyclbt.). More detail of the statistical analyses can be found in Table S1 in the ESI.†

Each of these two regressions represents an alternative rationale for the derivation of the chemical content of $4n/4n+2$ oligomers, which are both statistically relevant to the electronic excitability of the oligomers shown in Fig. 1.

The confidence interval of 95% associated with both approaches shows that all oligomers are within a statistical prediction band, leading to the quadratic equations (eqn (1) and (2)). These equations are useful for estimating the ratio between the $4n$ and $4n+2$ units required in order to approach a given gap width, when applied to oligomers with alternant chemistry as potential carbon-based nanowires.

We noted that the gaps of A, D, G and H are comparable to, or lower than those of other similar systems.[46] Indeed, the low HOMO–LUMO gaps show how changes in $4n/4n+2$ chemistries can affect the molecular conductive properties of such short oligomers, demonstrating the promise of this approach for the synthesis of equivalent polymeric systems. This is of particular interest, given the close relationship between the HOMO–LUMO gaps and the band-gaps of infinite polymers.[46]

This regression analysis gives an interesting though crude picture of how the alternation of $4n$ & $4n+2$ units in these oligomers can affect the molecular conductive properties by tuning the HOMO–LUMO gaps. However the relationship between the chemistry of the units and their tunability can be best answered by comparing the sequences of the oligomers.

**Table 1** HOMO–LUMO gaps and composition of the nine oligomers (ranked by excitability)

| Oligomer | Gap (eV) | $4n/4n+2$[a] | Napht./ben./cyclb. |
|---|---|---|---|
| A | 1.446 | 0.909 | 0.000 |
| H | 1.877 | 0.667 | 0.062 |
| G | 1.993 | 0.642 | 0.074 |
| D | 2.002 | 0.692 | 0.047 |
| E | 2.224 | 0.615 | 0.100 |
| I | 2.267 | 0.642 | 0.074 |
| C | 2.298 | 0.615 | 0.100 |
| F | 2.473 | 0.571 | 0.156 |
| B | 2.534 | 0.538 | 0.238 |

[a] Ratio between the counted number of cyclobutadiene and benzene rings.

### 3.3 Oligomer sequences and tunability

The sequence of the group of oligomers was investigated in order to derive a specific pattern between the sequence units and their effects on the electronic excitability of the oligomers. This is of particular importance, given that low currents are usually applied in the fields of optoelectronics, photonics and nanoelectronics. Under operation at low currents, different types of $4n/4n+2$ oligomers (and hence their polymer analogues) can therefore potentially respond with different conductivity profiles, thus presenting alternatives free from the conventional use of transistor- and resistance-dependent solids and metals with lower tunability (if tunable at all).

When the sequences are subdivided into pairs, an increasing number of NC pairs (naphthalene–cyclobutiadiene motif) seemingly increases the HOMO–LUMO gap (Table 2). Of particular interest, the molecular distance between NC motifs (assuming BC motifs are located in between) plays a potential role in the modulation of the HOMO–LUMO gap of these oligomers. This can be observed when the differences between

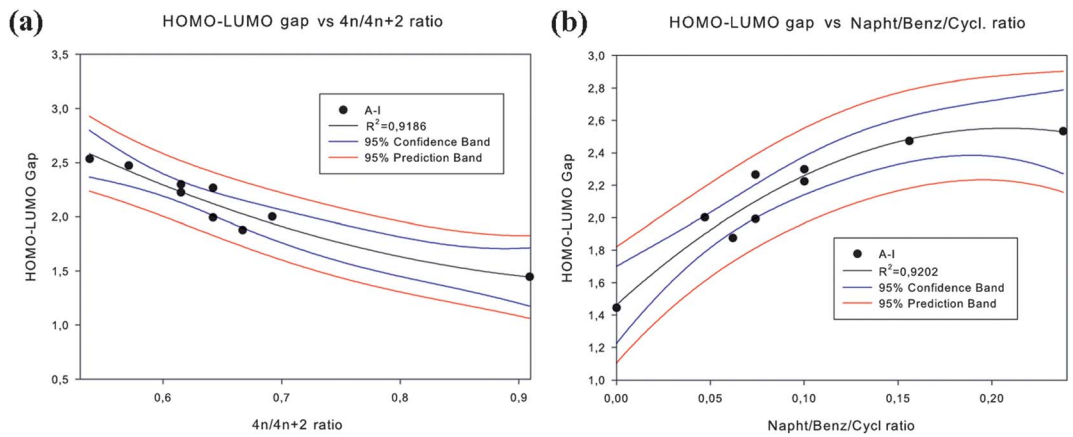


**Fig. 3** Statistical regression analysis of the quadratic correlation between the HOMO–LUMO gap and the chemical composition of the oligomers A–I. (a) HOMO–LUMO gap *versus* $4n/4n+2$ ratio. (b) HOMO–LUMO gap *versus* napht./benz/cyclbt. ratio.

**Table 2** Sequence and unit content of oligomers (ranked by excitability)[a]

| Oligomer | Sequence | % B | % N | % C | Gap (eV) | Δ |
|---|---|---|---|---|---|---|
| A | BC-BC-BC-BC-BC-BC-BC-BC-BC-B(…) | 52.3 | 0.0 | 47.7 | 1.446 | — |
| H | NC-BC-BC-BC-NC-BC-BC-BC-N(…) | 35.3 | 17.7 | 47.0 | 1.877 | 0.431 |
| G | NC-BC-BC-NC-BC-BC-NC-BC-BC-N(…) | 31.6 | 21.0 | 47.4 | 1.993 | 0.117 |
| D | BC-BC-NC-BC-BC-NC-BC-BC-NC-B(…) | 36.8 | 15.8 | 47.4 | 2.002 | 0.009 |
| E | BC-BC-NC-NC-BC-BC-NC-NC-B(…) | 29.4 | 23.5 | 47.1 | 2.224 | 0.222 |
| I | BC-BC-BC-NC-NC-NC-NC-BC-BC-B(…) | 31.6 | 21.0 | 47.4 | 2.267 | 0.042 |
| C | BC-NC-BC-NC-BC-NC-BC-NC-B(…) | 29.4 | 23.5 | 47.1 | 2.298 | 0.032 |
| F | BC-NC-BC-NC-NC-BC-NC-NC-B(…) | 23.5 | 29.4 | 47.1 | 2.473 | 0.175 |
| B | BC-NC-NC-BC-NC-NC-BC-N(…) | 20.0 | 33.3 | 46.7 | 2.534 | 0.060 |

[a] Benzene = B, naphthalene = N; cyclobutadiene = C. The sequence of units, *i.e.* CNCN, illustrates patterns of sequences that are repeated in alternative orders. The sequence and pattern composition is explored in order to find a rationale for the effect of the oligomer sequences on the HOMO–LUMO gap, along with the relative content of each unit (% B…). (…) illustrates the eventual repetition of the oligomer into polymers of $(\ldots)_n$ units. Δ is the difference between the HOMO–LUMO gaps from the previous oligomer ranked above.

HOMO–LUMO gaps are estimated between the oligomers (Table 2). In the case of oligomers E and D, where the difference between their HOMO–LUMO gaps is large ($\Delta = 0.222$ eV), oligomer E has two double NC units (contiguous NC pattern), which creates a large difference in the HOMO–LUMO gap in comparison to other pairs that do not have this difference in molecular sequence. This is also seen in the sequences of oligomers C and F, where their HOMO–LUMO gaps also have a large difference ($\Delta = 0.175$ eV), and oligomer F is differentiated from oligomer C by a double repetition of the NC pattern, as is the case in the E and D pair.

The repetition of units, pairs and motifs can thus be altered to tailor the sequences to yield desired conductivity/excitability ranges, facilitating studies *a priori* to band gap studies for the further synthesis of materials for potential application in nanoelectronic and microengineering circuits.

Sequencing in oligomer chemistry is a novel approach, given that sequencing is usually restricted to molecular and cellular biology. The concept of sequence motifs in oligomer chemistry presents a novel path in nanowire engineering and conductive molecular electronics. By changing the sequence order in oligomer-based wires, the motifs can induce a potential delay in the transfer of the electronic signal, particularly when working at ultra low voltages. The sequence can thus be an important factor for the design of tunable carbon-based linear molecular wires, through an approach of applying $4n/4n + 2$ oligomers of different gap widths (and sequence). The combination of the three unit types, benzene, naphthalene and cyclobutadiene, can thus be applied in molecular electronic devices, where $(NC)_n$ units function as semi-insulators and $(BC)_n$ units impart semiconductive properties.

Considering the oligomers presented herein, the largest difference in the HOMO–LUMO gap of 0.431 eV occurs between oligomers A and H, though structurally they only differ by two separated NC units. This large drop in excitability suggests that the sequence motif plays a key role in modulating the molecular electronic properties of such oligomer systems. The "sequence analysis" of the oligomers shows a pattern that suggests that the introduction of NC units has a potentially enormous effect on the molecular excitability pattern of these oligomers, and very probably on their corresponding $(NC)_n$ polymer analogues. The BC units possess excellent properties for reducing the HOMO–LUMO gaps, and indeed exhibit a pattern that can be further explored by wavefunction and orbital analysis. We therefore suggest that tunability can be putatively applied by the arrangement of pairs of sequences, in the ensemble of benzene, naphthalene and cyclobutadiene combinations (Table 2).

### 3.4 LUMO orbital morphology

During a conductive operation, the LUMOs are expected to play a central role by hosting the traveling electrons. In solids, the LUMOs of the atoms become the conducting band by merging into a contiguous super-orbital of higher energy than the HOMOs (valence band). In carbon-based conjugated systems, as in the case of the oligomers presented herein, electron transfer relies both on the LUMO and on the Fermi holes of the HOMOs during electron transport. The transfer of electrons across solids is instead determined by symmetry and by the distance between the atoms, with particular emphasis on overlapping s-orbitals.[47] In other words, for carbon-based conductors, electron transport becomes quite different given the bonded state of the carbon atoms. Studies by Yoshizawa, Tada and colleagues[48,49] have recently suggested a rationalization of the electron transport patterns in cyclic carbon-based molecules, based on solving the Landauer formula with Green's function.[50,51] Their studies have led to the development of an orbital rule for electron transport, which states that there are favorable and forbidden paths for an electron in order to travel through a carbon-based cyclic molecule.

In this context, we first analysed the LUMO morphologies of the nine oligomers (Fig. 1), which resulted in the identification of a potentially important relationship between the LUMO morphologies and the HOMO–LUMO gaps. Visual inspection shows a proposed rationale between the excitability levels and the number of homologue/heterologue symmetries of the LUMO elements, with their joined or separated arrangement and their respective wavefunction signs (Fig. 4). The profiling of LUMO orbitals indicates that the most conductive oligomers contain LUMO elements that are similar in shape and are

arranged in a symmetric fashion, as seen in the highly excitable oligomers A and H. The LUMO shapes also follow a parity principle, where large homologue pairs of opposite signs are located in contiguous large sections across the oligomer, without interruption. The degree of interruption in the morphological spatial distribution corresponds to the decreasing excitability of the oligomers, which suggests a rationale whereby the LUMOs obey a morphology rule for highly excitable oligomers which depends on the opposite signs occurring in pairs within the large LUMO sections (Fig. 4, red squares). In this pattern, the spatial occupancy of the LUMOs is also of particular interest, given that smaller and less homomorphic LUMO entities are found for less conductive/excitable oligomers. The gradual decrease in electronic excitability of the given oligomers is thus reflected by the LUMO elements becoming increasingly disjointed, or being governed by heteromorphic spatial distributions. The energy levels of the wavefunctions therefore appear to be dependent on being as similar as possible and having interchanging opposite wavefunction signs, in order to provide a conductive potential in such alternant carbon-based systems.

This interesting putative correlation between LUMO spatial distribution, the inter-orbital distances, and their repetitive or discontinuous patterns, can thus be an important quality/quantity to be considered in molecular conductance studies. Although conductance is not only attributed to the LUMO, and also involves charge-hopping transport, where the electron (LUMO to LUMO) or Fermi hole (HOMO/LUMO–LUMO/HOMO) hops, as well as the interchange of HOMO and LUMO during transport, a putative correlation (as observed) of the symmetric and geometric properties of orbitals in oligomers may add to the methodology of estimating the conductive properties of single molecules, oligomers and polymers. In parallel to the LUMO analysis, an analysis of the electron transport routes across the oligomers also gave interesting results for the further investigation of the conductive properties of $4n/4n + 2$ systems.

### 3.5 Electron distribution

The manner in which electrons are distributed in the alternant conjugated oligomers is also of crucial importance for the design of novel structures for sustainable nanowire technologies. To provide a deeper understanding of the electronic structure of the nine oligomers, we calculated the population number of π-electrons and the atomic charges for each of them. The results for two representative oligomers, A and F, are shown in Fig. 5, and the results for the remaining seven oligomers can be found in Fig. S3 (ESI†). The atomic numbering scheme is illustrated in Fig. 1.

From Fig. 5 as well as Fig. S3,† it can be seen that the distribution of both the π-populations and the atomic charges are remarkably uneven along the edge of the oligomers. From careful inspection of the figures, we report the following findings:

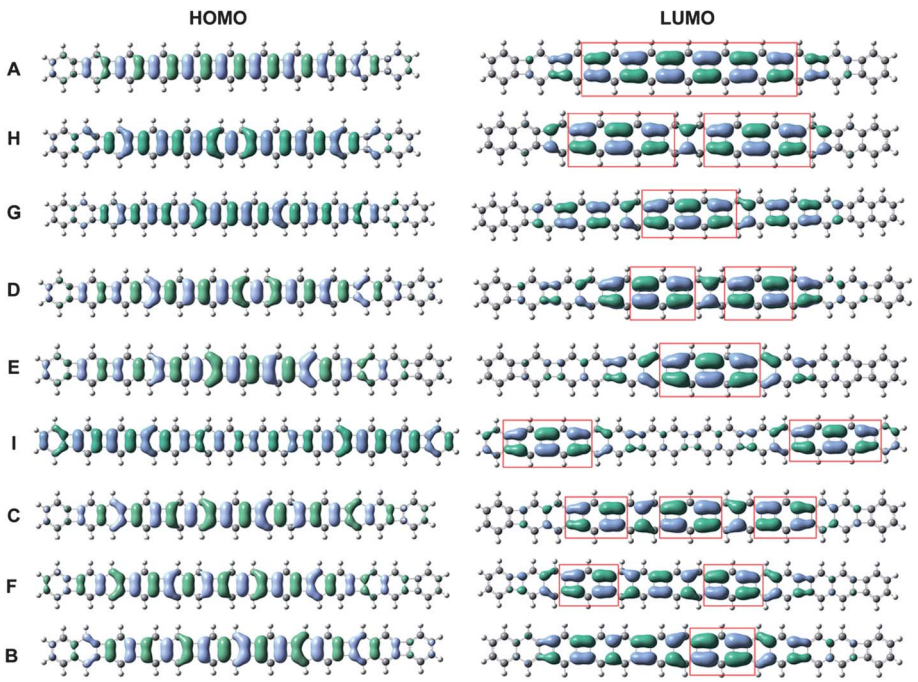


**Fig. 4** The HOMOs and LUMOs of the oligomers A–I. Accounting for the excitability values reported in Table 1, it is considered here that the spatial distribution of the LUMOs plays a significant role in the excitability of the oligomers. Upon inspection of the sequence of oligomers arranged by excitability from high to low, it can be see that the respective LUMO elements (highlighted by red squares) with similar symmetries indicate a putative relationship with the conductive properties, by their being adjacent to or separated from one another. The decreasing sequence of the oligomers' excitability and their LUMO components is as follows: A (6 joined coherent pairs of homomorphic LUMO elements) > H (2 separated units of 3 homomorphic elements) > G (1 unit of 3 homomorphic elements) > D (2 pairs of homomorphic elements) > E (1 unit of 3 homomorphic elements surrounded by LUMOs of highly different symmetries) > I (2 units of 3 homomorphic LUMO elements separated by ~7 Å) > C (3 pairs of homomorphic elements) > F (2 pairs separated by ~5 Å) > B (1 pair of homomorphic elements).

 

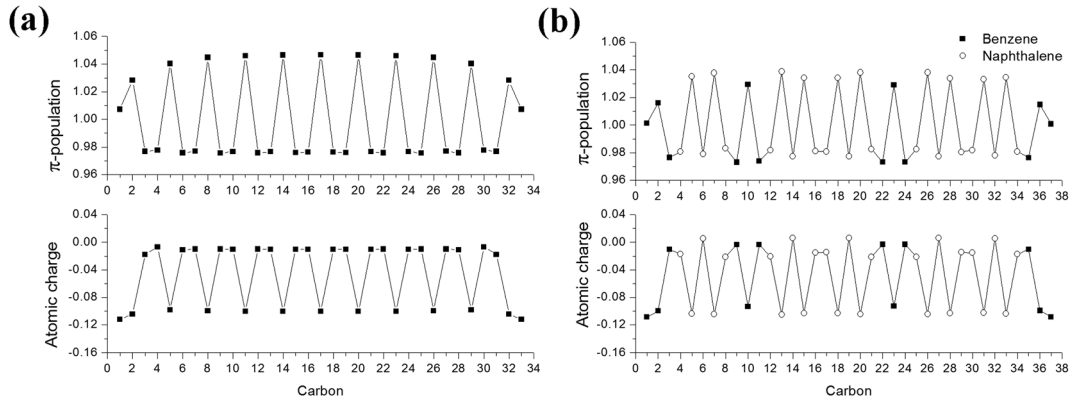


**Fig. 5** Population of π-electrons and atomic charges of the carbons in oligomer A (a) and in oligomer F (b). See Fig. S3 in ESI† for results of the other oligomers.

(1) The carbons at the middle of the $4n + 2$ rings always tend to have a relatively large number of π-electrons and possess an evident negative charge, irrespective of whether the ring is a benzene unit or part of a naphthalene unit. In contrast, π-electrons prefer not to reside on *either* the carbons in the cyclobutadiene units ($4n$) or those shared by the two $4n + 2$ rings (carbons in the middle of naphthalene units), and the atomic charges of these carbons are rather insignificant. This fluctuation of the π-population may be regarded as a result of the non-uniform electron delocalization over the oligomers (see later discussions).

(2) The π-population of the carbons in the $4n + 2$ rings of naphthalene units is always detectably larger than that of the corresponding carbons in the benzene units, regardless of the sequence of the oligomers. As a consequence, the former have a slightly more negative atomic charge than the latter (except for the carbons in the middle of the naphthalene units).

(3) Due to the limited lengths of the oligomers, the behavior of the carbons at the oligomer ends is different to the ones in the middle part; the fluctuation of the π-population at the two terminal carbons is evidently weakened. We also note that the two carbons closest to oligomer ends are often the mostly negatively charged.

Electrostatic potential (ESP)[52] measures the electrostatic interaction between a unit point charge placed at a specific point, and the system of interest. ESP distribution around the van der Waals (vdW) surfaces of molecules plays a crucial role in molecular packing in crystals and interactions with dopants. ESP maps above 1.7 Å (vdW radius of carbon) of the nine oligomer planes are given in Fig. S4 (ESI†). It can be seen that the ESP above the cyclobutadiene rings is negligible, *which implies a depletion zone of π-electrons*. The ESP value is negative above the benzene units, which can be explained by the abundance of π-electrons over the rings. Above the naphthalene units and especially above the terminal $4n + 2$ rings, the magnitude of the negative ESP is even larger, which can be well explained in terms of atomic charges, as discussed in points (2) and (3) (*vide supra*). A positive ESP only weakly occurs at the periphery of the oligomers, stemming mainly from the presence of positively charged hydrogen atoms.

### 3.6 Electron delocalization

The ability of electron delocalization, that is to say the conjugation efficiency, along the oligomers is inherently associated with their conductivity.[20] Since the strongly localized nature of σ-electrons results in their contributing little to the conductance, here we only focus on π-electron delocalization.

The isosurface map of the electron localization function for π-electrons (ELF-π)[53] of the two representative oligomers A and F are given in Fig. 6, where the isovalue is set to 0.5. The maps for the other oligomers can be found in Fig. S5 (ESI†). The isosurfaces of ELF-π clearly outline the favored channels of π-electron delocalization. It can be seen that in all oligomers, no prominent global delocalization channel is formed. π-electrons tend to delocalize within benzene or naphthalene units, and these domains of a high degree of delocalization are evidently separated by $4n$ units. Therefore, from a delocalization point of view, the presence of the $4n$ rings increases the number of electrons that are not subdivided into shells, which gives rise to the higher excitability.

Obviously, the ring geometries of benzene and naphthalene in the oligomer-state and in their free-state is different, owing to the constraint imposed by the neighbouring $4n$ units. In particular, from Fig. 6 and S5† it can clearly be seen that the hexagonal benzene rings in the oligomers are all compressed along the molecular axis. To quantitatively understand the impact of this ring deformation on electron delocalization, we calculated the six-membered bond order (6MBO) for each of the $4n + 2$ rings. 6MBO has been proven to be reliable in the measurement of aromaticity and electron delocalization.[54] The values are given underneath the isosurface maps in Fig. 6 and S5.† It can be seen that the terminal $4n + 2$ rings always have relatively larger 6MBOs and thus possess a higher extent of delocalization than the inner $4n + 2$ rings, the reason being that for terminal rings, the conformational constraint arising from neighbouring cyclobutadiene units is only exerted from one side rather than from both sides of the rings, and hence the resulting deviation from its ideal geometry will be less prominent. For the inner part of the oligomers, the 6MBOs of the rings in benzene units range from 0.057 to 0.061, while the 6MBOs of those in naphthalene units range from 0.038 to 0.045.

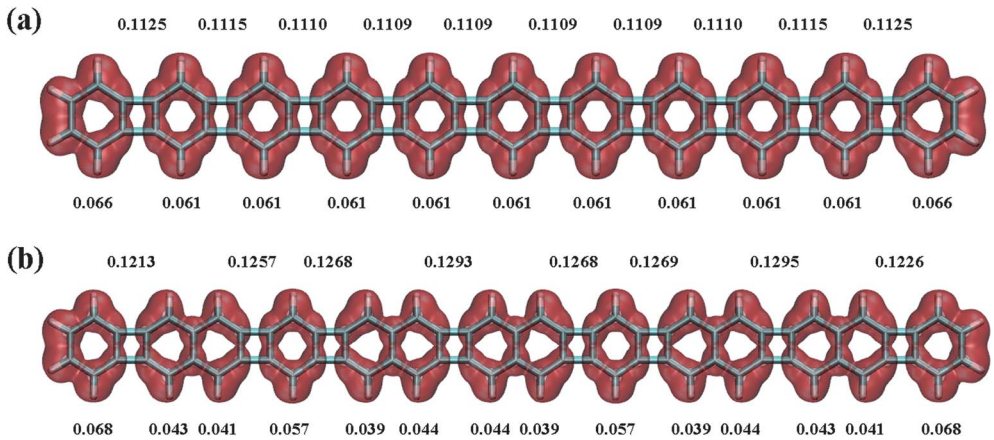


**Fig. 6** 0.5 isosurface of ELF-π: delocalization index of the horizontal C–C bonds in the 4*n* rings (top) and six-center bond order of the 4*n* + 2 rings (bottom) for oligomer A (a) and for oligomer F (b). See Fig. S5 in ESI† for results of the other oligomers.

In comparison, the 6MBOs for the rings in benzene and those in naphthalene in their free-states are 0.086 and 0.051, respectively. Apparently, the geometry deformation of the 4*n* + 2 rings in the *oligomer environment leads to a significant loss of delocalization momentum*.

The horizontal C–C bonds in the cyclobutadiene units (4*n*) behave as bridges, connecting the 4*n* + 2 units. The properties of these bonds were examined by the delocalization index for π-electrons (DI-π). The calculated values are given above the isosurface maps in Fig. 6 and S5.† Note that at the same calculation level, the DI-π values for the C–C bond in ethene and the one in benzene are 0.9348 and 0.4380, respectively. It can be seen that the DI-π values for the horizontal C–C bonds are rather small, ranging from 0.111 to 0.131, indicating that these bonds only have a weak π-component. In other words, π-electrons cannot delocalize very efficiently from one 4*n* + 2 unit to an adjacent one *via* these C–C bonds, strikingly delineating the energy barrier potential arising between the 4*n* + 2 and the 4*n* units, which can be exploited for semi-conducting tunability.

Accounting for the DI-π value being affected by the specific chemical environment, we find that its magnitude in general follows the given order: the C–C bond (4*n*) linking two naphthalene units > the C–C bond (4*n*) linking one benzene and one naphthalene unit > the C–C bond (4*n*) linking two benzene units. Seemingly, the presence of naphthalene units makes it easier for an electron to pass through a 4*n* unit, however this feature is not a determinant factor for controlling gaps.

To gain further insight, we also calculated the DI-π for the edge C–C bonds in the 4*n* + 2 units, and the results are summarized in Table S2.† Based on these data, we found a surprisingly large linear relationship between the DI-π and the HOMO–LUMO gaps, with an $R^2$ as high as 0.988:

$$\text{Gap (eV)} \approx -202.44 \times \overline{\text{DI}_{\pi}^{4n+2}} + 14.96 \times \overline{\text{DI}_{\pi}^{4n}} + 83.18 \qquad (3)$$

where $\overline{\text{DI}_{\pi}^{4n+2}}$ is the average value of the DI-π of the edge C–C bonds in 4*n* + 2 units, while $\overline{\text{DI}_{\pi}^{4n}}$ is that of the horizontal C–C bonds in the 4*n* units. The terminal benzene and naphthalene units were not taken into account. The scatter plot between the gaps predicted by this formula and the gaps calculated by B3LYP is shown in Fig. 7, and as can be seen, the prediction ability is rather satisfactory. It is worth noting that the trend in the variation of the DI-π values of the C–C bonds is very closely and linearly related with the bond lengths (see Fig. S6†). Therefore, in principle it is possible to reliably predict the oligomer gaps simply based on the optimized or experimentally determined geometry.

The coefficients in eqn (3) reveal that the average extent of the π-electron delocalization across the 4*n* + 2 rings is the dominant factor determining the HOMO–LUMO gaps; the higher the delocalization the narrower the gaps. Notice that the average DI-π of the edge C–C bonds in the naphthalene units is smaller than that of the edge C–C bonds in the benzene units, which explains our aforementioned finding that wider gaps are observed in the oligomers containing higher numbers of naphthalene units. In contrast to the 4*n* + 2 units, the delocalization behavior in the 4*n* units evidently has less influence on the gaps; the higher the ability of the π-electrons to

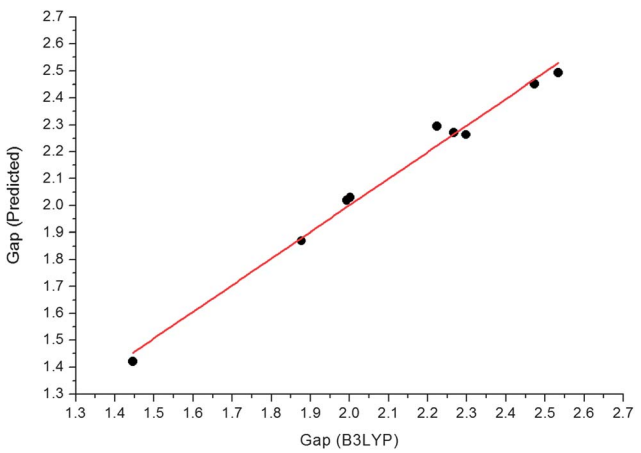


**Fig. 7** The scatter plot between the gaps predicted by eqn (3) and the gaps derived from B3LYP calculation.

 

delocalize through the $4n$ units, the wider the gaps. We have mentioned that $\overline{DI_{\pi}^{4n+2}}$ and $\overline{DI_{\pi}^{4n}}$ are generally inversely correlated with each other, which implies that there may be a competitive relationship between intra-unit and inter-unit delocalization of the $4n + 2$ units, emphasizing the significant role of $4n/4n + 2$ linear systems in tuning the conductivity in nanoelectronic circuits.

## 4 Conclusions

The quantum chemical analysis of the oligomers presented herein suggests that the $4n$ content in the $4n/4n + 2$ alternant conjugated oligomers, is responsible for the observed narrow HOMO–LUMO gaps, and is thus expected to be the most significant contributor to the conductive properties in their corresponding polymers. This statement is supported by the interdependent relationship found between oligomers and polymers in similar studies.[42,46] The initial analysis presented herein also shows that the aromatic units in the oligomeric structures are a base for expanding HOMO–LUMO gaps, and can be used to tune the semi-conductance and resistivity of the final full-scale polymers. Alternating $4n/4n + 2$ chemistry in different ratios can therefore give various semi-conductive properties, and can be used as a base strategy for the development of novel carbon-based conductive and semi-conductive materials for application in microelectronic technologies. The alternation of the chemical content ($4n$ or $4n + 2$) can thus play a role in the design of tunable molecular nanowires, with desired conductances.

Furthermore, a potential correlation between the symmetries of adjacent orbitals at the LUMO level may explain the conductive properties of the oligomers presented herein, assuming a direct relationship between the HOMO–LUMO gap and the band gap.[46]

Finally, the electron distributions and electron delocalizations of the oligomers were explored in detail. The results show that the distribution of $\pi$-electrons is evidently uneven, preferentially residing in the $4n + 2$ rings rather than the $4n$ rings, which is the main source of the non-uniformity of the electrostatic potential distributed on the oligomer vdW surfaces. The $\pi$-electron delocalization in the oligomers was characterized by means of ELF-$\pi$, six-center bond order and delocalization index. We found that the $4n$ units somewhat hindered the passing of electrons through the entire oligomer. The presence of the $4n$ units led to a great loss of delocalization momentum of the benzene rings in the oligomers, due to their resulting severe geometric deformation. Moreover, a striking relationship was found between the HOMO–LUMO gap and the $\pi$-delocalization index of the C–C bonds along the molecular axis, which correlated well with one another.

## Acknowledgements

The authors would like to thank Prof. van Der Spoel at the University of Uppsala, Computational Systems and Biology, for kindly supplying hardware and software for calculations under the guest-researcher position.

## References

1 X. Guo, H. Li, B. Yeop Ahn, E. B. Duoss, K. J. Hsia, J. A. Lewis and R. G. Nuzzo, *Proc. Natl. Acad. Sci. U. S. A.*, 2009, **106**, 20149–20154.
2 F. J. Beck, S. Mokkapati and K. R. Catchpole, *Opt. Express*, 2011, **19**, 25230–25241.
3 B. Tian, X. Zheng, T. J. Kempa, Y. Fang, N. Yu, G. Yu, J. Huang and C. M. Lieber, *Nature*, 2007, **449**, 885–889.
4 J. Tang, Z. Huo, S. Brittman, H. Gao and P. Yang, *Nat. Nanotechnol.*, 2011, **6**, 568–572.
5 M. Law, L. E. Greene, J. C. Johnson, R. Saykally and P. Yang, *Nat. Mater.*, 2005, **4**, 455–459.
6 A. Tanaka, *Toxicol. Appl. Pharmacol.*, 2004, **198**, 405–411.
7 R. W. Miles, K. M. Hynes and I. Forbes, *Prog. Cryst. Growth Charact. Mater.*, 2005, **51**, 1–42.
8 C. K. Chiang, M. A. Druy, S. C. Gau, A. J. Heeger, E. J. Louis, A. G. MacDiarmid, Y. W. Park and H. Shirakawa, *J. Am. Chem. Soc.*, 1978, **100**, 1013–1015.
9 R. F. Curl and R. E. Smalley, *Science*, 1988, **242**, 1017–1022.
10 C. M. Varma, J. Zaanen and K. Raghavachari, *Science*, 1991, **254**, 989–992.
11 S. Iijima and T. Ichihashi, *Nature*, 1993, **363**, 603–605.
12 X.-X. Zhang, S.-P. Cheng, C.-J. Zhu and S.-L. Sun, *Pedosphere*, 2006, **16**, 555–565.
13 Y. Zhao, B. L. Allen and A. Star, *J. Phys. Chem. A*, 2011, **115**, 9536–9544.
14 C. K. Chiang, C. R. Fincher, Jr, Y. W. Park, A. J. Heeger, H. Shirakawa, E. J. Louis, S. C. Gau and A. G. MacDiarmid, *Phys. Rev. Lett.*, 1977, **39**, 1098–1101.
15 H. Shirakawa, E. J. Louis, A. G. MacDiarmid, C. K. Chiang and A. J. Heeger, *J. Chem. Soc., Chem. Commun.*, 1977, **0**, 578–580.
16 Y. Sun, N. C. Giebink, H. Kanno, B. Ma, M. E. Thompson and S. R. Forrest, *Nature*, 2006, **440**, 908–912.
17 X. Wang, K. Maeda, X. Chen, K. Takanabe, K. Domen, Y. Hou, X. Fu and M. Antonietti, *J. Am. Chem. Soc.*, 2009, **131**, 1680–1681.
18 M. Alcarazo, *Dalton Trans.*, 2011, **40**, 1839–1845.
19 Y. Yang, Y. Lu, M. Lu, J. Huang, R. Haddad, G. Xomeritakis, N. Liu, A. P. Malanoski, D. Sturmayr, H. Fan, D. Y. Sasaki, R. A. Assink, J. A. Shelnutt, F. van Swol, G. P. Lopez, A. R. Burns and C. J. Brinker, *J. Am. Chem. Soc.*, 2003, **125**, 1269–1277.
20 S. Manzetti, in *Nanoscience & Computational chemistry: Research Progress*, ed. E. A. Castro, A. K. Haghi and A. Mercader, CRC Press Taylor and Francis, 2013, ch. 5.
21 M. Randić, *Chem. Rev.*, 2003, **103**, 3449–3606.
22 Y. Aoki, A. Imamura and I. Murata, *Tetrahedron*, 1990, **46**, 6659–6672.
23 Y. Sugihara, H. Yamamoto, K. Mizoue and I. Murata, *Angew. Chem., Int. Ed. Engl.*, 1987, **26**, 1247–1249.
24 A.-R. Allouche, *J. Comput. Chem.*, 2011, **32**, 174–182.
25 M. J. Frisch, G. W. Trucks, H. B. Schlegel, G. E. Scuseria, M. A. Robb, J. R. Cheeseman, J. A. Montgomery, Jr, T. Vrevon, K. N. Kudin, J. C. Burant, J. M. Millam, S. S. Iyengar, J. Tomasi, V. Barone, B. Menucci, M. Cossi,

G. Scalmani, N. Rega, G. A. Petersson, H. Nakatsuji, M. Hada, M. Ehara, K. Toyota, R. Fukuda, J. Hasegawa, M. Ishida, T. Nakajima, Y. Honda, O. Kitao, H. Nakai, M. Klene, X. Li, J. E. Knox, H. P. Hratchian, J. B. Cross, C. Adamo, J. Jaramillo, R. Gomparts, R. E. Stratmann, O. Yazyev, A. J. Austin, R. Cammi, C. Pomelli, J. W. Ochterski, P. Y. Ayala, K. Morokuma, G. A. Voth, P. Salvador, J. J. Dannenberg, V. G. Zakrzewski, S. Dapprich, A. D. Daniels, M. C. Strain, O. Farkas, D. K. Malick, A. D. Rabuck, K. Raghavachari, J. B. Foresman, J. V. Ortiz, Q. Cui, A. G. Baboul, S. Clifford, J. Cioslowski, B. B. Stefanov, G. Liu, A. Liashenko, P. Piskorz, I. Komaromi, R. L. Martin, D. J. Fox, T. Keith, M. A. Al-Laham, C.-Y. Peng, A. Namayakkara, M. Challacombe, P. M. W. Gill, B. Johnson, W. Chen, M.-W. Wong, C. Gonzalez and J. A. Pople, *Gaussian 03, E.01*, Gaussian, Inc., Wallingford, CT, 2004.

26 A. D. Becke, *J. Chem. Phys.*, 1993, **98**, 1372–1377.

27 P. C. Hariharan and J. A. Pople, *Theor. Chem. Acc.*, 1973, **28**, 213–222.

28 W. J. Hehre, R. Ditchfield and J. A. Pople, *J. Chem. Phys.*, 1972, **56**, 2257–2261.

29 A. D. Becke, *J. Chem. Phys.*, 1993, **98**, 5648–5652.

30 J. P. Perdew, K. Burke and M. Ernzerhof, *Phys. Rev. Lett.*, 1996, **77**, 3865–3868.

31 C. Adamo and V. Barone, *J. Chem. Phys.*, 1998, **108**, 664–675.

32 M. J. Frisch, J. A. Pople and J. S. Binkley, *J. Chem. Phys.*, 1984, **80**, 3265–3269.

33 Xplot website: http://www.xplot.org (accessed on 31, Mar, 2013).

34 T. Lu and F. Chen, *J. Comput. Chem.*, 2012, **33**, 580–592.

35 R. S. Mulliken, *J. Chem. Phys.*, 1955, **23**, 1841–1846.

36 T. Lu and F. Chen, *J. Theor. Comput. Chem.*, 2012, **11**, 163–183.

37 T. Lu and F. Chen, *Acta Phys.–Chim. Sin.*, 2012, **28**, 1–18.

38 X. Fradera, M. A. Austen and R. F. W. Bader, *J. Phys. Chem. A*, 1998, **103**, 304–314.

39 F. W. Bader, *Atoms in Molecules: A Quantum Theory*, Oxford University Press, New York, 1994.

40 E. Matito, J. Poater, M. Solà, M. Duran and P. Salvador, *J. Phys. Chem. A*, 2005, **109**, 9904–9910.

41 R. Ponec and I. Mayer, *J. Phys. Chem. A*, 1997, **101**, 1738–1741.

42 S. Yang, P. Olishevski and M. Kertesz, *Synth. Met.*, 2004, **141**, 171–177.

43 S. S. Zade, N. Zamoshchik and M. Bendikov, *Acc. Chem. Res.*, 2010, **44**, 14–24.

44 M. Kertesz, S. Yang and Y. Tian, in *Handbook of thiophene-based materials: Applications in organic electronics and photonics*, ed. I. F. Perepichka and D. F. Perepichka, John Wiley & Sons Ltd, Chichester, 2009, vol. 1, ch. 7, pp. 341–364.

45 W. J. Yu, L. Liao, S. H. Chae, Y. H. Lee and X. Duan, *Nano Lett.*, 2011, **11**, 4759–4763.

46 M. Chattopadhyaya, S. Sen, M. M. Alam and S. Chakrabarti, *J. Chem. Phys.*, 2012, **136**, 094904–094909.

47 P. Atkins and R. Friedman, *Molecular quantum mechanics*, Oxford University Press Oxford, New York, 2010.

48 K. Yoshizawa, T. Tada and A. Staykov, *J. Am. Chem. Soc.*, 2008, **130**, 9406–9413.

49 K. Yoshizawa, *Acc. Chem. Res.*, 2012, **45**, 1612–1621.

50 R. Landauer, *IBM J. Res. Dev.*, 1957, **1**, 223–231.

51 S. Datta, *Electronic transport in mesoscopic systems*, Cambridge University Press, Cambridge, 1997.

52 J. S. Murray and P. Politzer, *WIREs Comput. Mol. Sci.*, 2011, **1**, 153–163.

53 J. C. Santos, W. Tiznado, R. Contreras and P. Fuentealba, *J. Chem. Phys.*, 2004, **120**, 1670–1673.

54 M. Giambiagi, M. S. de Giambiagi, C. D. dos Santos Silva and A. P. de Figueiredo, *Phys. Chem. Chem. Phys.*, 2000, **2**, 3381–3392.

 